A 3D simulation of the formation of primary platelet thrombi based on a hybrid computational model

Chaoqing MA, Oubong GWUN*

Division of Computer Science and Engineering, Faculty of Engineering, Chonbuk National University, Jeonju-si, Jeollabuk-do, Republic of Korea

Abstract: Recently, the study of thrombosis simulation based on computational models has been one of the most popular research areas. In this paper, a 3D simulation method based on a hybrid model is proposed for platelet thrombus formation. The flow of platelets is modeled in a macroscale submodel using Navier–Stokes equations and the physiological processes such as adhesion and aggregation of platelets are modeled in a microscale submodel. In the adhesion and aggregation phases, the attraction of platelets due to blood coagulation factors (von Willebrand factor) is modeled using the external force, and the conversion from unstable aggregation to stable aggregation is modeled using the increase in local viscosity. The proposed model is implemented and is applied to the 3D simulation of platelet thrombus formation. The flow of platelets and the transformation from normal platelet to thrombus are well shown by the 3D view of the simulation. The velocity field and viscosity field are also rendered to observe their changes in the process of thrombus formation. In the simulation, as the increase in blood velocity, the primary thrombus grows rapidly before a velocity threshold, and then the growth rate decreases. It concurs with the experimental results in vivo.

Key words: Platelet thrombus formation, three-dimensional simulation, hybrid model, level sets

1. Introduction

Thrombi are clots anchored to vascular walls containing blood cells and fibrous proteins, and the process of thrombus formation is called thrombosis. Thrombosis may cause myocardial infarction and stroke, which are diseases causing severe disability and high death rates [1–3]. Therefore, research on thrombus formation is important for thrombosis prevention and treatment. In recent years, the simulation of thrombus formation by computer technology has become one of the new directions in thrombus research. In the simulation of thrombus formation, the flow of blood and the interaction between blood cells, fibrous proteins, and vascular walls are modeled using a computational model based on hemodynamics and biomechanical processes. The thrombus formation models are implemented and visualized using computer technology. It is obvious that this type of thrombus formation simulation has the advantages of convenience and cost saving compared with experiments carried out in the laboratory.

The simulation of thrombus formation has been proposed in numerous papers [4–21]. Thrombus simulation can be classified into mixed thrombus simulation or platelet thrombus simulation according to the type of thrombus ingredient to be simulated. The mixed thrombus is a blood clot with platelets, white cells, red cells, and fibrous proteins, while the primary platelet thrombus only contains platelets. Since the platelet thrombus

is the basic form of the mixed thrombus, the platelet thrombus research is as significant as the mixed thrombus research. The performance of platelets in thrombus formation has been well understood in physiology and biochemistry [22–26]. Fogelson and Neeves also give us a review of the experimental and modeling research of blood clot formation concentrating on platelets and von Willebrand factor (vWf) [4]. The models of platelet transport, margination, adhesion, and aggregation are discussed as an important part of thrombus formation model in their paper.

Kamada et al. proposed a series of multiscale models for platelet thrombus formation [9–11]. The flow of plasma and platelets is modeled by the moving particle semi-implicit (MPS) method in macroscale and the motion of the adhered and aggregated platelets is modeled by mechanical spring forces in microscale. The hybrid DPD-PDE model proposed by Tosenberger et al. uses dissipative particle dynamics (DPD) to model plasma flow and platelets, and the regulatory network of plasma coagulation is modeled by a system of partial differential equations (PDEs) [13]. The models above are all based on the discrete particle system, but in many other models only the platelets are modeled as discrete particles while the plasma is modeled as a continuum material. The multiscale models proposed by Xu et al. and used in their papers [14–17] are formed by the macroscale model describing the dynamics of the blood flow in continuum Navier–Stokes (N-S) equations and the microscale model describing the interactions among platelets, fibrins, and the vascular wall in an extended stochastic discrete cellular Potts model (CPM). Sweet et al. developed a new subcellular element Langevin (SCEL) model [18] in which the cell motion and deformation are simulated by SCE and the cells are coupled to the continuum plasma by the Langevin equation. The problems that should be solved in building a model for thrombus formation simulation are the balance between calculation amount and calculation accuracy, and the determination of platelet size. In the discrete particles-based models, since the computation amount and accuracy are controlled by the particles number and size, the platelet size should match the computing requirements. Moreover, in the models in which each cell is formed by lattices and the accuracy of computation is determined from the size of lattices, the size of the cells should therefore be large enough to contain more than 1 lattice. In Skorczewski et al.'s paper [19], they suppose a method in which each platelet and blood cell is represented by a set of discrete Lagrangian points and moving through the Cartesian grid containing fluid velocity information.

In this paper, a 3D simulation for the formation of platelet thrombi is proposed. The simulation is based on a hybrid computational model in which the hemodynamics of blood flow is modeled by N-S equations in the macroscale submodel and adhesion and aggregation of platelets are modeled in the microscale submodel by applying forces to platelets and changing the viscosity of platelets. One of the innovative points of this model is that the reversible and irreversible aggregation are modeled by local viscosity change combined with boundary conditions that fits the feature of the N-S equation and can be implemented easily. Another innovative point is that in the model N-S equations are solved using level set methods and the marker-and-cell (MAC) grid. Platelets move according to the velocity field stored in the MAC grid. The model enables any computation accuracy to be obtained by controlling the MAC grid resolution, and the number and the size of platelets are independent.

2. Hybrid model of platelet thrombus formation

The formation of platelet thrombi occurs from the process involving platelets adhering to the injured endangium and platelets aggregating together. Here, we assume that platelets are small particles flowing uniformly inside the vessel. Each platelet has its own speed composed of normal speed $\vec{u}_{\text{normal}}$ obtained from the macroscale

submodel and the acceleration $\vec{a}_{platelet}$ from the microscale submodel:

$$\vec{u}_{platelet} = \vec{u} + \Delta t \, \vec{a}_{\text{platelet}} \tag{1}$$

2.1. Macroscale submodel

Since we assumed the blood flow to be a type of incompressible viscose Newton fluid, the blood flow is specified using continuum N-S equations:

$$\frac{\partial \vec{u}}{\partial t} + \vec{u} \bullet \nabla \vec{u} + \frac{1}{\rho} \nabla p = \vec{a} + \nu \nabla \bullet \nabla \vec{u} \tag{2}$$

$$\nabla \bullet \vec{u} = 0 \tag{3}$$

Eq. (2) is the momentum equation showing how the fluid flows under the influences of pressure p, acceleration $\vec{a}$, and kinematic viscosity ν. In the equation, $\vec{u}$, t, and ρ are the fluid velocity, time, and fluid density, respectively. Eq. (3) shows the incompressibility condition ensuring the fluid is incompressible.

All the variables in the N-S equations are stored in a MAC grid (Figure 1) [27]. The MAC grid is not only a Cartesian grid but is also a staggered grid. One of its features is that different variables are arranged at different locations. The 3 components of velocity u, v, and w are at the center of each cell face. Viscosity is at each cell corner and pressure is at the cell center. For the cell with index (i, j, k), the variables take the index while adding or subtracting $\frac{1}{2}$ from (i, j, k), so that they can indicate their locations in the cell.
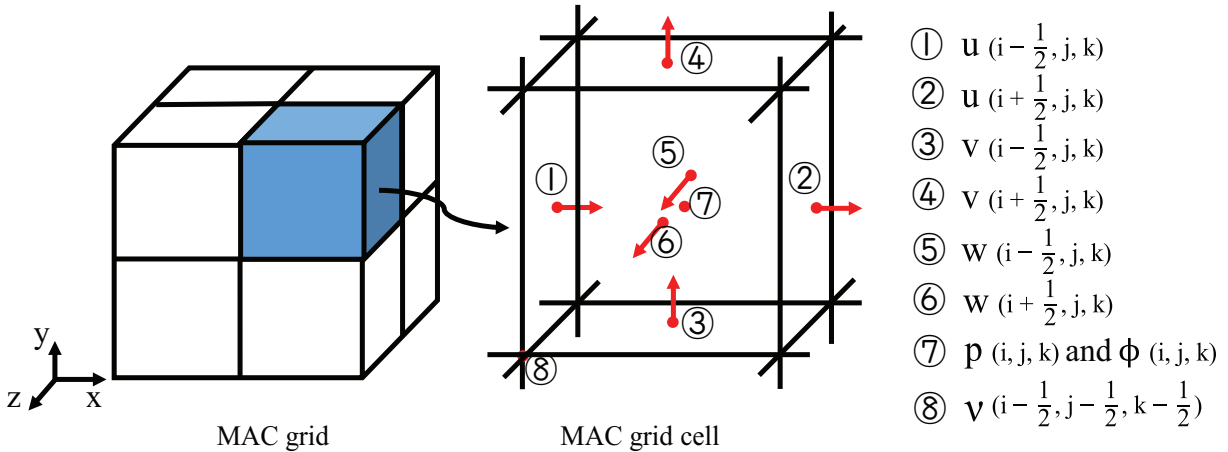

① $u_{(i-\frac{1}{2}, j, k)}$
② $u_{(i+\frac{1}{2}, j, k)}$
③ $v_{(i-\frac{1}{2}, j, k)}$
④ $v_{(i+\frac{1}{2}, j, k)}$
⑤ $w_{(i-\frac{1}{2}, j, k)}$
⑥ $w_{(i+\frac{1}{2}, j, k)}$
⑦ $p_{(i, j, k)}$ and $\phi_{(i, j, k)}$
⑧ $v_{(i-\frac{1}{2}, j-\frac{1}{2}, k-\frac{1}{2})}$

MAC grid   MAC grid cell

Figure 1. Example of MAC grid arrangement.

Depending on the N-S equations, the pressure gradient is subtracted from the interim velocity $\vec{u}'$ to ensure the velocity field satisfies the incompressibility condition:

$$\vec{u}^n = \vec{u}' - \Delta t \, \frac{1}{\rho} \nabla p \tag{4}$$

The MAC grid provides an accurate central difference because, for each velocity component at the cell face, there are 2 pressure values at the center of either cell sharing this face. Eq. (4) for the u, v, and w velocity components can be written as

$$\vec{u}^{n}_{i+\frac{1}{2},\,j,\,k} = \vec{u}'_{i+\frac{1}{2},\,j,\,k} - \Delta t\, \frac{1}{\rho}\, \frac{p_{i+1,j,k} - p_{i,j,k}}{\Delta x} \tag{5}$$

$$\vec{v}^{n}_{i,\,j+\frac{1}{2},\,k} = \vec{v}'_{i,\,j+\frac{1}{2},\,k} - \Delta t\, \frac{1}{\rho}\, \frac{p_{i,j+1,k} - p_{i,j,k}}{\Delta y} \tag{6}$$

$$\vec{w}^{n}_{i,\,j,\,k+\frac{1}{2}} = \vec{w}'_{i,\,j,\,k+\frac{1}{2}} - \Delta t\, \frac{1}{\rho}\, \frac{p_{i,j,k+1} - p_{i,j,k}}{\Delta z} \tag{7}$$

The surface function $\phi(\vec{x})$ is defined as level sets and is used to distinguish the blood area from the nonblood area. It is also stored at the cell center of the MAC grid. The surface of blood is represented by $\phi(\vec{x}) = 0$, and so the area inside the blood has $\phi(\vec{x}) < 0$ and the area outside the blood has $\phi(\vec{x}) > 0$. This is because the vessel is full of blood; before the thrombus arises, the vascular wall is the interface where the level set is zero and the region inside the vascular wall is blood while the region outside the vascular wall is nonblood. The surface function is calculated from the signed distance function [28]:

$$\phi(\vec{x}) = \begin{cases} distance\,(\vec{x}) \ : \vec{x}\,is\,outside \\ -distance\,(\vec{x}) \ : \vec{x}\,is\,inside \end{cases} \tag{8}$$

$$distance\,(\vec{x}) = \|\vec{x} - \vec{p}\|, \tag{9}$$

where $\vec{p}$ is a point on the interface closest to $\vec{x}$. During the formation of the platelet thrombus, the interface between the blood and nonblood areas expands into the vessel. The $\phi(\vec{x})$ values are updated after each interface change.

On the interface, the boundary conditions should be defined. For a point on the interface, its velocity is divided into a normal component and a tangential component as shown in Figure 2a, where $\hat{n}$ and $\hat{t}$ are the normal unit vector and tangential unit vector, respectively. In the inviscid case, we assume that the boundary condition on the interface is related to the no-stick boundary condition:

$$\vec{u}_{no-stick} \bullet \hat{n} = \vec{u}_{nonblood} \bullet \hat{n} \tag{10}$$
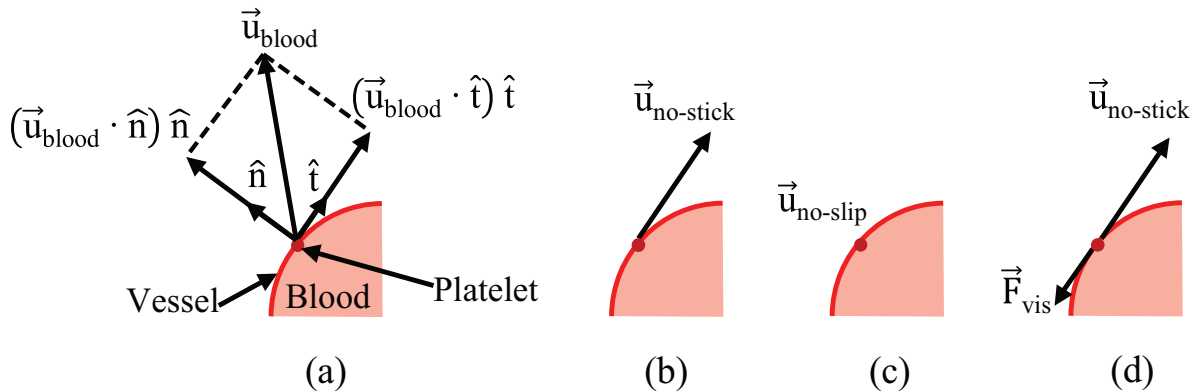

Figure 2. Boundary conditions on a curving boundary. (a) is blood velocity decomposition. (b) is velocity under no-stick boundary condition. (c) is velocity under no-slip boundary condition. (d) is boundary condition used in this paper.

The normal component of the blood velocity on the vascular wall ($\vec{u}_{no-stick}$) is matched with the normal component of the nonblood velocity ($\vec{u}_{nonblood}$), which is zero in our case (Figure 2b). In the viscous case, according to the no-slip boundary condition:

$$\vec{u}_{no-slip} = \vec{u}_{nonblood} \tag{11}$$

the tangential component of blood velocity is zero (Figure 2c). Since blood is a viscous fluid, the vascular wall and the thrombus surface are not coarse surfaces. Instead of using this no-stick or no-slip boundary condition directly, we define a force $\vec{F}_{vis}$:

$$\vec{F}_{vis} = -\rho\,D\,\vec{u}_{no-stick} \tag{12}$$

where D is a coefficient proportional to the viscosity value (Figure 2(d)). We use $\frac{\vec{F}_{vis}}{\rho}$ as an acceleration to reduce $\vec{u}_{no-stick}$ to 0 after some time steps:

$$\vec{u}^n = \vec{u}_{no-stick} + \frac{\Delta t}{\rho}\,\vec{F}_{vis}, \tag{13}$$

where $\vec{u}_{no-stick}$ is equal to the tangential component of $\vec{u}_{blood}$ in the last time step and $\vec{u}^n$ is the velocity of the current step. These are decreased sequentially to finally reach 0. The boundary condition is applied to the interface where the level set is zero. From the definition of the signed distance function, the gradient of ϕ is the direction towards the closest point on the interface; the normal of the interface is thus equal to $\nabla\phi$. By taking advantage of the level sets, the calculation of $\hat{n}$ becomes easier, especially in the case of a surface with an irregular shape during the growth of a thrombus.

Platelets achieve their normal velocity by interpolating the velocity in their center of gravity from the velocity field, which is the result of the solution of N-S equations.

2.2. Microscale submodel

The injured endangium is one of the causes of thrombosis. In the primary stage, the coagulation system is activated by the exposed collagen and tissue factors. Then, with the intervention of the vWf, the platelets adhere to the injured endangium. Finally, the stuck platelets release materials to force more platelets to aggregate together. Platelet adhesion and aggregation are the main parts of the platelet thrombus formation. We model these 2 phases in microscale from the external force and the increase in local viscosity.

In the platelet adhesion, we use an adhesion radius R_{ad} to define the area affected by vWf. Only the platelet in this area and not adhered to the injured endangium can be affected by vWf. The intervention of vWf is modeled by a force from the injured endangium acting on the platelets. Figure 3 is an illustration of platelet adhesion. We make an adhesion shell with the radius R_{ad} around a platelet. The injured endangium inside the shell is the adhesion surface S_{ad}, and the adhesion force of platelet i located in (x_i, y_i, z_i) is the integral of $f(x, y, z)$ on S_{ad}. The adhesion forces $\vec{F}_{adhesion}$ along the x, y, z axis are

$$F_x = \int_{S_{ad}} f(x, y, z) \times \frac{(x - x_i)}{d(x, y, z)}\,dS \tag{14}$$

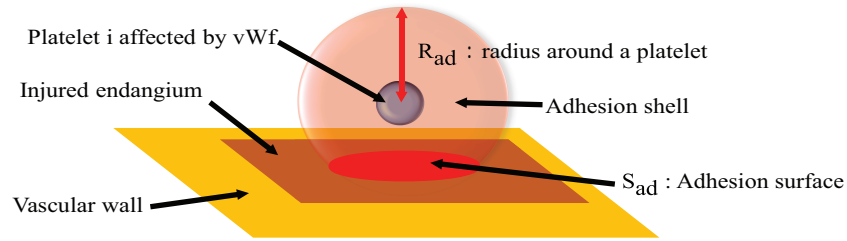$$F_y = \int_{S_{ad}} f(x, y, z) \times \frac{(y - y_i)}{d(x, y, z)}\,dS \tag{15}$$

Figure 3. Illustration of platelet adhesion.

$$F_z = \int_{S_{ad}} f\,(x,\,y,\,z) \times \frac{(z - z_i)}{d(x,\,y,\,z)}\,dS, \tag{16}$$

where $f\,(x,\,y,\,z)$ is the force from a point $(x,\,y,\,z)$ on the adhesion surface:

$$f\,(x,\,y,\,z) = \frac{F_{\max}\,(R_{ad} - d\,(x,\,y,\,z))}{R_{ad}}, \tag{17}$$

where $F_{\max}$ is the maximum of the adhesion force and $d(x,\,y,\,z)$ is the distance between the platelet i and a point $(x,\,y,\,z)$. $f\,(x,\,y,\,z)$ is in inverse proportion to the distance from the injured wall. This adhesion force provides acceleration with the platelets:

$$\vec{a}_{\text{platelet}} = \frac{1}{\rho}\,\vec{F}_{adhesion} \tag{18}$$

where $\vec{a}_{\text{platelet}}$ and ρ are the acceleration and blood density, respectively. The attracted platelet gets close to the injured endangium or the growing thrombus under the adhesion force.

The exposed collagen fibers on the injured endangium and ADP, TXA2, 5-HT, etc. released by platelets promote platelet adhesion and aggregation. We model this process by increasing the local viscosity on the surface of injured endangium and thrombus from normal viscosity ν_{nor} to injured endangium viscosity ν_{ing}. That means if the cell of the MAC grid contains the surface of injured endangium or thrombus, the viscosity values on the corners are ν_{ing}. When the surface of an attracted platelet is located on the MAC cell containing the surface of injured endangium, we think that the attracted platelet touches the injured endangium, and this platelet becomes a part of the thrombus. As a joint result of the boundary conditions (Eqs. (12) and (13)) and increased local viscosity, this platelet is captured and slows down. At the same time, the viscosity of the cell containing captured platelet surface and injured endangium and the cell of the platelet interior increases to aggregation viscosity ν_{agg} to quicken the stopping of the platelet. Since the platelet surface except the touch part has become thrombus surface, the viscosity values should increase to ν_{ing}. In the aggregation phase, the captured platelet is initially unstable and reversible. After this platelet is activated, the aggregation becomes stable and irreversible. In this model, before the speed of the captured platelet becomes zero, there is still a possibility that the captured platelet breaks off from the thrombus, which is seen as the reversible state. The state changes from reversible to irreversible when the platelet speed becomes zero and stops on the thrombus or the injured endangium completely.

3. 3D simulation based on hybrid model

We apply the above proposed hybrid model to the simulation of platelet thrombus formation in a vessel. The vessel and platelet are designed as shown in Figure 4. Our virtual vessel is designed as a straight tube. We

embed the tube into a box called a MAC grid box, which is used to build a MAC grid. n_i, n_j, and n_k are the resolutions of the MAC grid referring to the number of cells into which the box is divided on the x, y, and z axes. The direction of blood flow is from left to right. The width (W_b) and length (L_b) of the MAC grid box are $50\,\mu m$ and $200\,\mu m$, respectively. The diameter (D_v) and length (L_v) of the vessel are $20\,\mu m$ and $200\,\mu m$, respectively. The injured endangium is at the end part of the vessel with a length $L_i = 20\,\mu m$ and central angle $\theta_i = \frac{\pi}{4}$. We approximate the platelets with spheres with a diameter $D_p = 2\,\mu m$. We assume that there are 200 platelets in the vessel and about 32 particles per $10^4\,\mu m^3$. The number of platelets and their diameters are not the same as those of the platelets in a venule, but are suitable for simulation and visualization in the thrombus formation study. In each frame, there are platelets flowing out the vessel or transforming to thrombus. Thus we count the number of remaining platelets and add appropriate number of platelets from the inflow to keep the number of platelets flowing inside the vessel fixed. In the initialization step, the locations of platelets in the whole vessel are assigned randomly, and the new platelets of each frame are located randomly in the empty area before the old platelet closest to the vessel entry.
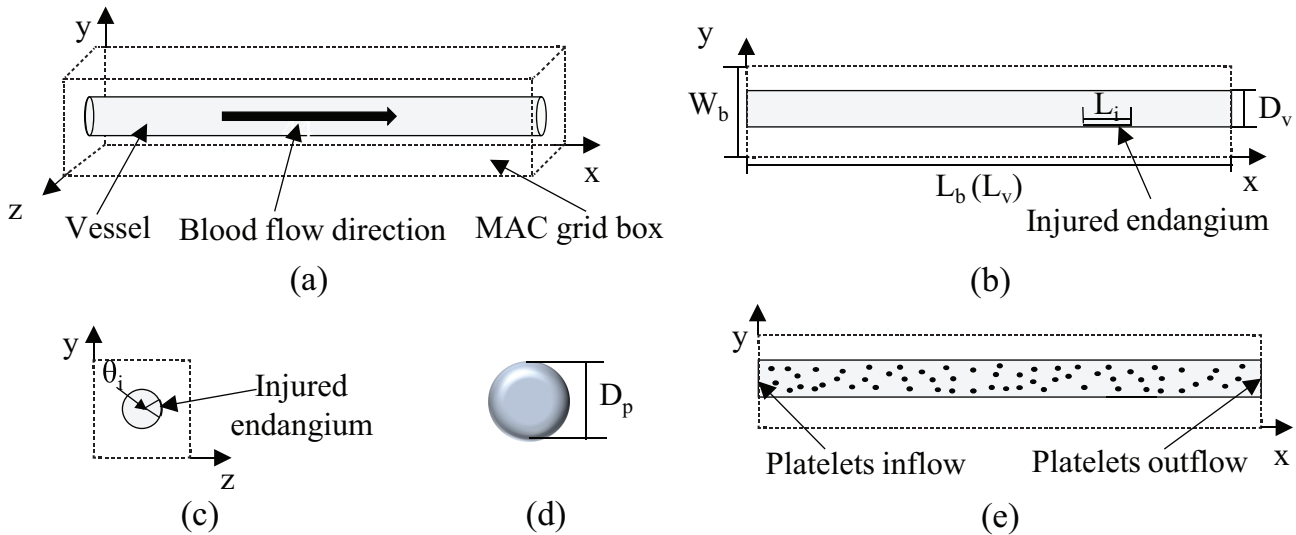

Figure 4. Design of virtual vessel and blood flow. (a) is 3D view of virtual vessel. (b) is section cut from z axis. (c) is section cut from x axis. (d) is virtual platelet. (e) is platelets flow in the virtual vessel.

The simulation process is summarized in the flow chart below in Figure 5. In the initialization, the initial platelets position, initial velocity, initial viscosity, and level sets are set up. The time for 1 frame (frame time) consists of dozens of time steps and the N-S equations in the macroscale submodel are solved by the loop at every time step. After 1 frame time, the velocities of the platelets are calculated from the velocity field. The accelerations of the platelets are calculated from the adhesion force and are then added to the velocities of the platelets. Then the platelets move according to these velocities. Again, the viscosities in the platelet thrombus are increased and are used as the viscosities in the next frame. Finally, the location of every normal platelet and stuck platelet, the velocity field, and the viscosities are obtained from the simulation results. In the simulation, 40 s are costed for 1 frame averagely. More than 80% of that time is used to solve N-S equations for blood flow simulation. Note that adhesion force computation, platelet advection, and viscosity increase take less time because they are applied not for every time step but for every time frame. This method reduces the simulation time at the slight cost of simulation accuracy.
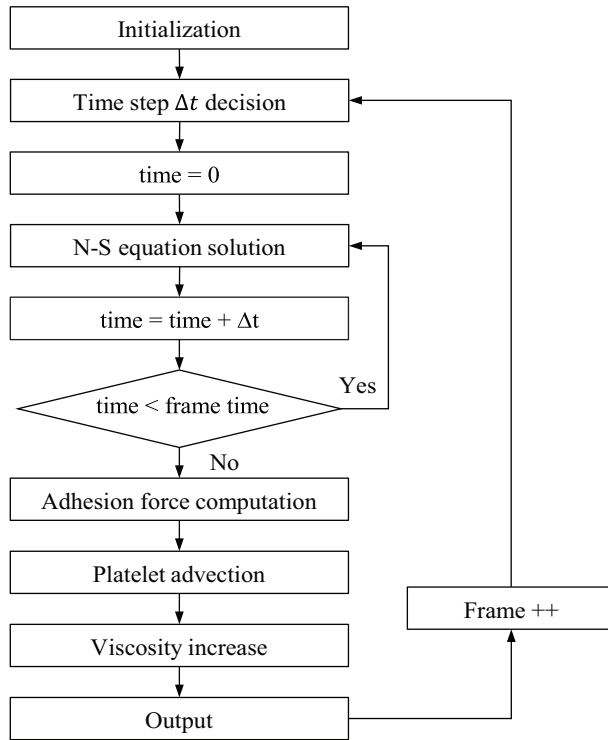
Figure 5. Flow chart of the 3D simulation.

4. Experimental results

We implemented the hybrid model proposed in section 2 in Windows platform and applied it to simulate the formation of primary thrombus in 3D. The implementation of a fluid flow simulation based on level set methods is referenced from Batty's fluid 3D framework [29]. The average values of hemodynamics and the simulation parameters are listed in Tables 1 and 2.

Table 1. Average values of hemodynamics.

Parameter	Value
Blood flood velocity	$2\,mm/s$
Reynolds number	0.01
Vessel diameter	$20\,\mu m$

Table 2. Values of simulation parameters.

Parameter	Value		
D	$50\,\nu$		
Time/frame	1×10^{-3} s		
$n_i \times n_j \times n_k$	$30 \times 120 \times 30$		
R_{ad}	10 μm	20 μm	
F_{max}	0.2 N	0.4 N	
ν_{inj}	5 pa·s	10 pa·s	20 pa·s
ν_{agg}	50 pa·s	100 pa·s	200 pa·s
ρ	1 g/cm^3		

The development process of the platelet thrombus formation and the change process of viscosity are visualized as shown in Figure 6 using VTK. Figure 6a illustrates a series of frames for platelets adhesion and aggregation at different times with an initial blood velocity of $2\,mm/s$. In each frame, the platelets affected by the vWf are shown in light green, the aggregated platelets are shown in red, and the normal platelets are shown in blue. The red platelets form the primary thrombus. Because the platelets aggregate together by platelet surface without platelet deformation, the thrombus seems loose before a large amount of platelets are aggregated. Because almost all of the platelets passing the injured endangium are affected by vWf and adhere to the thrombus, with platelets flowing out of the vessel, there are a few platelets in the end part of the vessel at time $t = 0.3\,s$. Figure 6b shows the change process of viscosities. The region in red indicates the part with normal viscosity. The orange region represents the thrombus surface with viscosity value ν_{inj}. The purple region represents the thrombus interior with viscosity value ν_{agg}. The growth of the thrombus results in a high viscosity region extension.
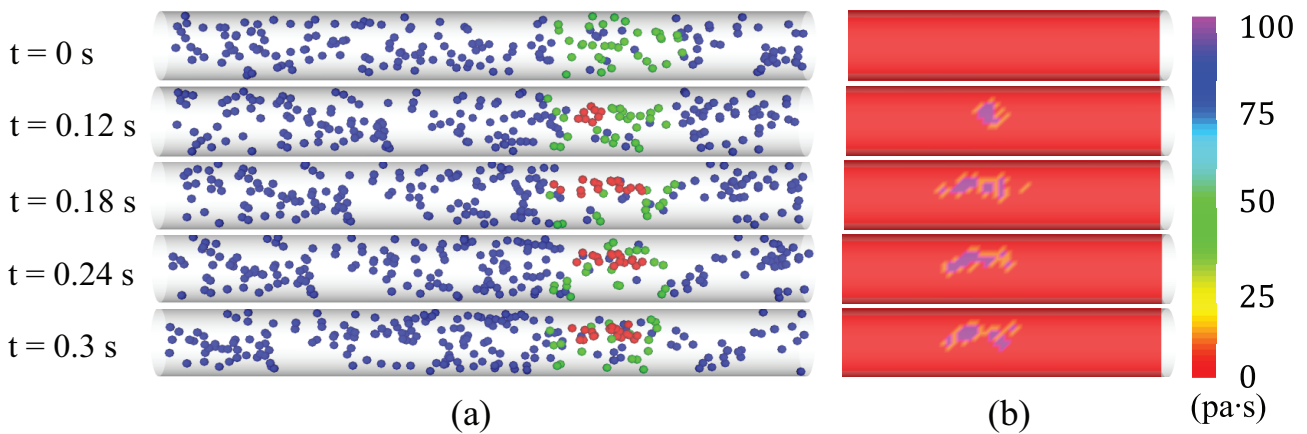

Figure 6. (a) is frames of platelet thrombus formation in the injured vessel. The platelets affected by the vWf are shown in light green, the aggregated platelets are shown in red. (b) is viscosity values of section cut from z = 0.25 with initial blood velocity of 2 mm/s.

We also visualized the velocity field in the vessel as shown in Figure 7. In the MAC grid, the 3 velocity components are stored at different faces of a cell, so that we can obtain the velocity vector at the cell center by interpolation. For visualizing the entire region affected by vWf, we combine the normal speed $\vec{u}_{normal}$ and the acceleration $\vec{a}_{platelet}$ of the platelet located in the cell center. In the region far from the injured endangium, the velocities are almost the same as the initial blood velocity (Figure 7a). However, for the region closer to the injured endangium, the velocities' vector gradually points toward the injured part. Therefore, the platelets in this region move toward the injured endangium and the thrombus. In this region, the number of velocities pointing to the injured endangium increases as the point approaches the injured endangium. This is because the adhesion force in the microscale submodel is in inverse proportion to the distance from the injured endangium. However, the velocities simultaneously slow down. This is because the thrombus region has zero velocity. The high viscosity around the thrombus reduces the speed of the nearby velocities. Increasingly more velocities slow down with the growth of the thrombus (Figure 7b).

The velocity of blood flow is one of the most important influential factors in thrombus formation. We performed the simulation with different velocities of blood flow to analyze the relationship between primary
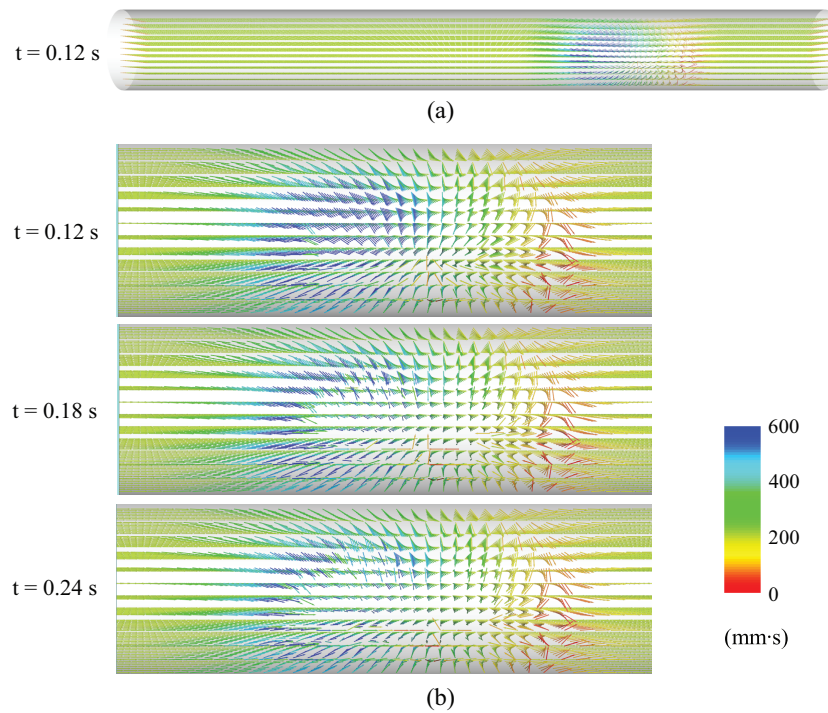
Figure 7. Velocity fields with the initial velocity of 2 mm/s. (a) is velocity field of the whole vessel. (b) is velocity fields near the injured endangium.

thrombus formation and blood flow velocity. The growth rates of the primary thrombus are shown in Figure 8. Figure 8a shows the results where $R_{ad} = 10\,\mu m$ and $F_{\max} = 0.2\,N$. Figure 8b shows the results where $R_{ad} = 20\,\mu m$ and $F_{\max} = 0.4\,N$. In both cases, the growth rate increases as velocity increases, until the velocity reaches a threshold. After that, the growth rate decreases. These results agree with the in vivo experiment result of Begent and Born's study [21]. Their results are shown in Figure 8c. The results are the white thrombus (platelet thrombus) growth rates in golden hamsters with the vessel diameters of $50 \sim 69\,\mu m$. Before the threshold value of blood velocity is reached, the platelet thrombus grows rapidly by increasing the blood velocity. This is because more platelets pass the injured endangium in unit time. However, when the blood velocity is greater than the threshold value, the platelets exit before adhering to the injured endangium or stuck platelets; moreover they detach from the thrombus even after they have become aggregated. The influence of vWf grows with the increase in R_{ad} and $F_{\max}$. Since the R_{ad} and $F_{\max}$ shown in Figure 8b are 2 times those shown in Figure 8a, the growth rate shown in Figure 8a is much lower than that shown in Figure 8b, and the threshold increases from $1.5\,mm/s$ to $3.5\,mm/s$. We also varied the values of ν_{ing} and ν_{agg} for the local viscosity in the region of the platelet thrombus. The simulation results in Figure 9 show that, if blood velocities are the same, the thrombus with high local viscosity grows more rapidly than that with low local viscosity. Although the blood brings the same number of platelets under the same blood velocity, the high local viscosity forces the platelets influenced by vWf to slow down and stop easily, and fewer platelets are washed away by blood before the aggregation becomes stable.

5. Conclusion

In this paper, a hybrid model is proposed for the 3D simulation of platelet thrombus formation. A macroscale submodel is used to model the blood flow based on N-S equations. In this model, N-S equations are solved
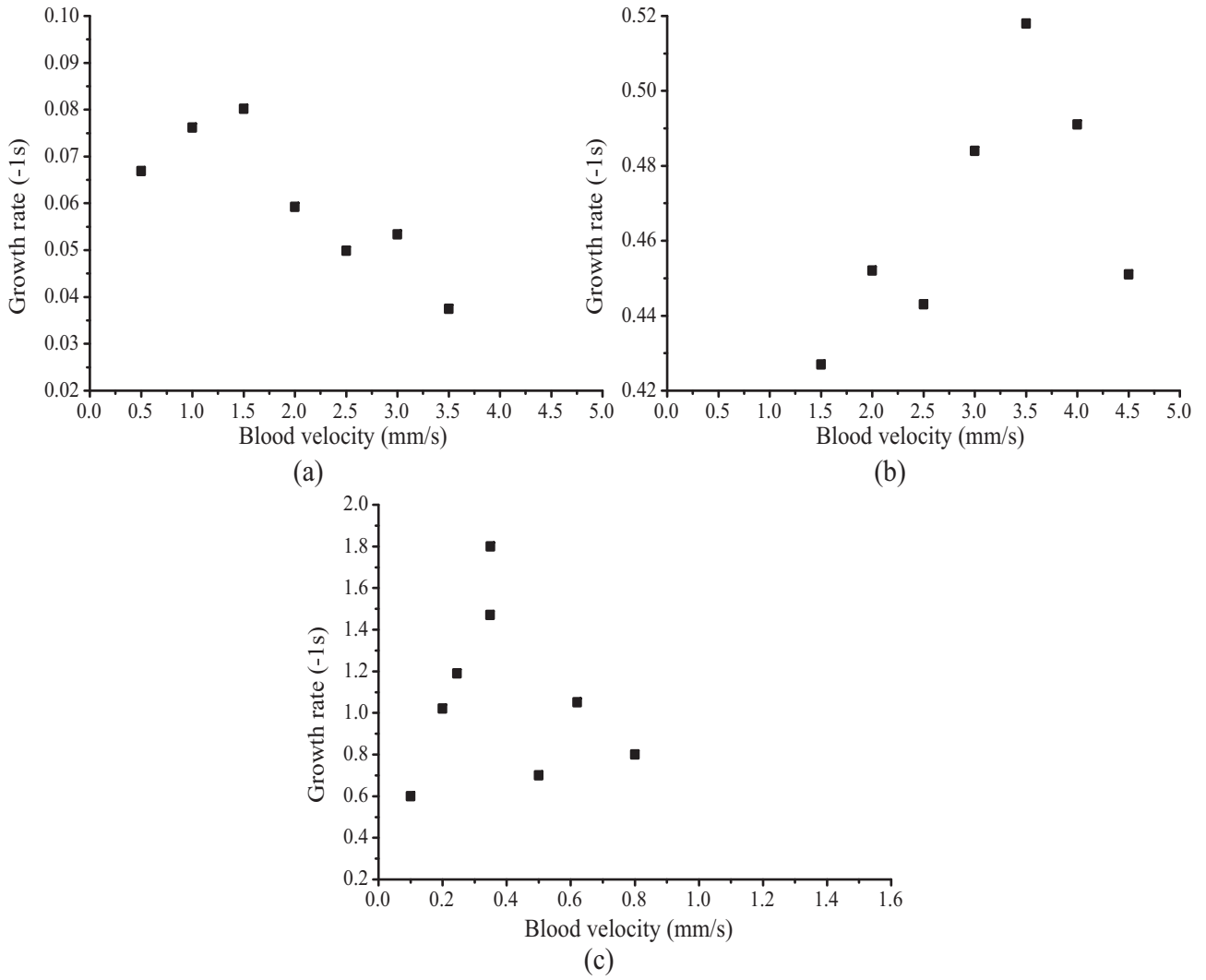
Figure 8. Growth rates of the platelet thrombus formation in different velocities. (a) and (b) are our simulation results with $R_{ad} = 10\,\mu m$, $F_{max} = 0.2\,N$ and $R_{ad} = 20\,\mu m$, $F_{max} = 0.4\,N$, respectively. (c) is the result Begent and Born's study [16].
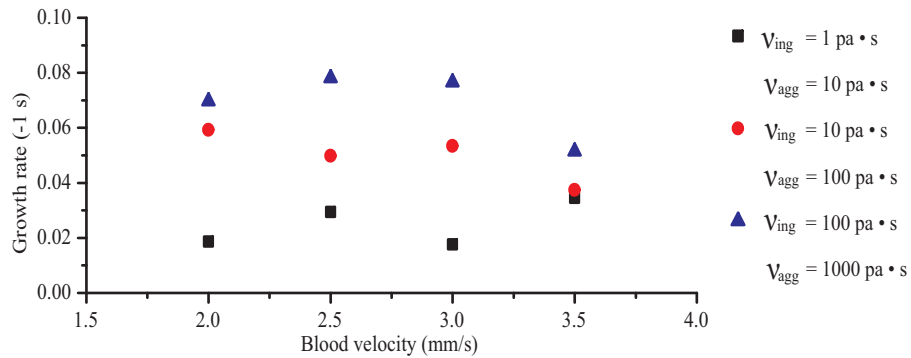

Figure 9. Growth rates of the platelet thrombus with different local viscosities.

using level set methods and a MAC grid. The level sets help to distinguish the blood region from the nonblood region and the MAC grid makes adjustments of computational accuracy based on grid resolution without the need to change the platelet particle size. The microscale submodel is used for the reactions between the normal platelets, stuck platelets, and injured endangium. This submodel is built using the external force acting on the platelets and the increase in local viscosity.

We apply this hybrid model to the 3D simulation of the platelet thrombus. From the 3D simulation, we can observe the growth of the platelet thrombus including platelets, adhesion, and aggregation. The simulations are carried out at different velocities to analyze the relationship between the platelet thrombus formation and the blood velocity. The results show that the rate of thrombus growth increases as the blood velocity increases before the velocity reaches a threshold. After that, the growth rate reduces as the blood velocity increases. We also test the varying local viscosity values, and reach the conclusion that high local viscosity leads to high thrombus growth rate.

The computational model-based simulation of blood clot formation is an efficient way to understand the thrombosis mechanism. The 3D simulation proposed in this paper is a new attempt at modelling thrombus by level sets and MAC grid in the hybrid model. One of the advantages of this model is that it opens the possibility of simulating on the vessel with complex geometries. The other one is that it frees the platelet size from the calculating accuracy. However, the proposed model is still an imperfect model with weaknesses. For example, the time-cost in the blood flow

References

[1] Fuster V, Badimon L, Cohen M, Ambrose JA, Badimon JJ, Chesebro J. Insights into the pathogenesis of acute ischemic syndromes. Circulation 1988; 7: 1213-1220.

[2] Fuster V, Badimon L, Badimon JJ, Chesebro JH. The pathogenesis of coronary artery disease and the acute coronary syndromes-part I. New Engl J Med 1992; 326: 242-250.

[3] Fuster V, Badimon L, Badimon JJ, Chesebro JH. The pathogenesis of coronary artery disease and the acute coronary syndromes-part II. New Engl J Med 1992; 326: 310-318.

[4] Fogelson AL, Neeves KB. Fluid mechanics of blood clot formation. Annu Rev Fluid Mech 2015; 47: 377-403.

[5] Weller FF. A free boundary problem modeling thrombus growth: model development and numerical simulation using the level set method. J Math Biol 2010; 61: 805-818.

[6] Fogelson AL, Guy RD. Platelet-wall interactions in continuum models of platelet thrombosis: formulation and numerical solution. Math Med Biol 2004; 21: 293-334.

[7] Miyazaki H, Yamaguchi T. Formation and destruction of primary thrombi under the influence of blood flow and von Willebrand factor analyzed by a discrete element method. Biorheology 2003; 40: 265-572.

[8] Mori D, Yano K, Tsubota K, Ishikawa T, Wada S, Yamaguchi T. Computational study on effect of red blood cells on primary thrombus formation. Thromb Res 2008; 123: 114-121.

[9] Kamada H, Tsubota K, Nakamura M, Wada S, Ishikawa T, Yamaguchi T. A three-dimensional particle simulation of the formation and collapse of a primary thrombus. Int J Numer Meth Biomed Eng 2010; 26: 488-500.

[10] Kamada H, Tsubota K, Nakamura M, Wada S, Ishikawa T, Yamaguchi T. Computational study on effect of stenosis on primary thrombus formation. Biorheology 2011; 48: 99-114.

[11] Kamada H, Imai Y, Nakamura M, Ishikawa T, Yamaguchi T. Computational study on thrombus formation regulated by platelet glycoprotein and blood flow shear. Microvasc Res 2013; 89: 95-106.

[12] Tosenberger A, Ataullakhanov F, Bessonov N, Panteleev M, Tokarev A, Volpert V. Modelling of thrombus growth and growth stop in flow by the method of dissipative particle dynamics. Russ J Numer Anal M 2012; 27: 1-16.

[13] Tosenberger A, Ataullakhanov F, Bessonov N, Panteleev M, Tokarev A, Volpert V. Modelling of platelet-fibrin clot formation in flow with a DPD-PDE method. J Math Biol 2016; 72: 649-681.

[14] Xu Z, Alber M, Chen N, Kamocka MM, Rosen ED. A multiscale model of thrombus development. J Roy Soc Interface 2008; 5: 705-722.

[15] Xu Z, Alber M, Chen N, Shadden SC, Marsden JE, Kamocka MM, Rosen ED, Alber M. Study of blood flow impact on growth of thrombi using a multiscale model. Soft Matter 2009; 5: 769-779.

[16] Xu Z, Lioi J, Mu J, Kamocka MM, Liu X, Chen DZ, Rosen ED, Alber M. A multiscale model of venous thrombus formation with surface-mediated control of blood coagulation cascade. Biophys J 2010; 98: 1723-1732.

[17] Xu Z, Christley S, Lioi J, Kim O, Harvey C, Sun W, Rosen ED, Alber M. Multiscale model of fibrin accumulation on the blood clot surface and platelet dynamics. Methods Cell Biol 2012; 110: 367-388.

[18] Sweet CR, Chatterjee S, Xu Z, Bisordi K, Rosen ED, Alber M. Modelling platelet–blood flow interaction using the subcellular element Langevin method. J R Soc Interface 2011; 8: 1760-1771.

[19] Skorczewski T, Erickon LC, Fogelson AL. Platelet motion near a vessel wall of thrombus surface in two-dimensional whole blood simulations. Biophys J 2013; 104: 1864-1772.

[20] Filipovic N, Kojic M, Tsuda A. Modelling thrombosis using dissipative particle dynamics method. Philos T Roy Soc A 2008; 336: 99-106.

[21] Cito S, Mazzeo MD, Badimon L. A review of macroscopic thrombus modeling methods. Thromb Res 2013; 131: 116-124.

[22] Begent N, Born GVR. Growth rate in vivo of platelet thrombi, produced by iontophoresis of ADP, as a function of mean blood flow velocity. Nature 1970; 227: 926-930.

[23] Schmugge M, Rand ML, Freedman J. Platelets and von Willebrand factor. Transfus Apher Sci 2003; 28: 269-277.

[24] Jurk K, Kehrel BE. Platelets: physiology and biochemistry. Semin Thromb Hemost 2005; 31: 381-392.

[25] Furie B, Furie BC. In vivo thrombus formation. J Thromb Haemost 2007; 1: 12-17.

[26] Furie B, Furie BC. Mechanisms of thrombus formation. New Engl J Med 2008; 395: 938-949.

[27] Bridson R. Fluid Simulation for Computer Graphics. Wellesley, MA, USA: A K Peters, Ltd., 2008.

[28] Osher S, Fedkiw R. Level Set Methods and Dynamic Implicit Surfaces. New York, NY, USA: Springer-Verlag, 2003.

[29] Batty C, Bridson R. Accurate viscous free surfaces for buckling, coiling, and rotating liquids. In: The ACM SIGGRAPH/Eurographics Symposium on Computer Animation; 07–09 July 2008; Dublin, Ireland. New York, NY, USA: ACM SIGGRAPH. pp. 219-228.